Acta Crystallographica Section D
Biological Crystallography
ISSN 0907-4449

Structural studies of human insulin cocrystallized with phenol or resorcinol *via* powder diffraction

Fotini Karavassili,[a] Anastasia E. Giannopoulou,[a] Eleni Kotsiliti,[a] Lisa Knight,[b] Mathias Norrman,[c] Gerd Schluckebier,[c] Lene Drube,[c] Andrew N. Fitch,[b] Jonathan P. Wright[b] and Irene Margiolaki[a]*

[a]Department of Biology, Section of Genetics, Cell Biology and Development, University of Patras, 26500 Patras, Greece, [b]European Synchrotron Radiation Facility, BP 220, 38043 Grenoble CEDEX 9, France, and [c]Diabetes Protein Engineering, Novo Nordisk A/S, Novo Nordisk Park, 2760 Måløv, Denmark

Correspondence e-mail: imargiola@upatras.gr

Received 1 August 2012
Accepted 14 September 2012

The effects of the ligands phenol and resorcinol on the crystallization of human insulin have been investigated as a function of pH. Powder diffraction data were used to characterize several distinct polymorphic forms. A previously unknown polymorph with monoclinic symmetry ($P2_1$) was identified for both types of ligand with similar characteristics [the unit-cell parameters for the insulin–resorcinol complex were a = 114.0228 (8), b = 335.43 (3), c = 49.211 (6) Å, β = 101.531 (8)°].

1. Introduction

Insulin is a small protein built up of two chains which are linked to each other by two disulfide bridges. It is first synthesized as pre-insulin in β-cells located in the pancreas (Itoh & Okamoto, 1980; Leibowitz *et al.*, 2002). Owing to its biological function (Banting & Best, 1922), this hormone is used in the medical treatment of diabetes. The primary administration route is by subcutaneous injection of microcrystals or mixtures of microcrystals and amorphous protein. After injection, the insulin crystals dissolve slowly, thus leading to a gradual release of insulin into the bloodstream (Norrman & Schluckebier, 2007). A crystallographic structure of insulin was first determined in 1969 (Adams *et al.*, 1969). Since then, a number of polymorphs have been identified that crystallize in various space groups, with the most common belonging to the monoclinic, rhombohedral, cubic and tetragonal crystal systems (Norrman, 2007, PhD thesis). The determination of the type, size and morphology of the crystals is crucial, as these characteristics affect the speed at which insulin is released into the bloodstream (Norrman & Schluckebier, 2007). Nowadays, the use of insulin microcrystals in new administration approaches, such as pulmonary delivery, is of great interest in order to improve treatments for diabetes (Basu *et al.*, 2004).

Powder diffraction has previously been exploited as a technique for fingerprinting different crystalline forms of human insulin and has allowed the rapid phase identification and quantification of mixtures (Norrman *et al.*, 2006). High-resolution powder instrumentation is designed to obtain the sharpest possible diffraction peaks in reciprocal space and also to determine accurate peak positions (Margiolaki *et al.*, 2007; Wright *et al.*, 2008). These features are complementary to area-detector single-crystal experiments, where the aim is normally to measure diffraction peaks at the highest possible scattering angles in order to improve the direct-space resolution in an electron-density map.

The first protein structure refinements and solutions *via* the molecular-replacement method using powder data were reported by Von Dreele (Von Dreele, 1999; Von Dreele *et al.*,

2000). The use of high-resolution synchrotron data together with new analysis procedures has made powder crystallography a powerful complementary method for structural characterization of proteins (Basso *et al.*, 2005; Margiolaki *et al.*, 2005, 2007; Margiolaki & Wright, 2008; Collings *et al.*, 2010). Microcrystalline powders can be obtained for many proteins by batch precipitation (Von Dreele, 2003), which is of great advantage, as growing a suitable single crystal is often a more demanding procedure. Thus, powder methods are ideal for the systematic study of crystallization conditions as it is possible to characterize microcrystalline precipitates. However, in the powder technique there is a severe loss of information owing to the collapse of the three-dimensional diffraction pattern onto a single dimension with accompanying overlap of Bragg peaks, which becomes progressively worse at higher scattering angles and complicates structural analysis in comparison to single-crystal methods.

In this paper, we employed synchrotron X-ray powder diffraction to investigate the effect of pH on the crystallization of human insulin with two different ligands: phenol and resorcinol. Phenol and phenol-like compounds were originally added to insulin preparations as antibacterial agents. It turns out that phenol binds to the insulin hexamer and has a dramatic effect on the insulin conformation, driving it into the R state (Derewenda *et al.*, 1989). The presence of zinc is crucial to the formation and stability of the insulin hexamer, whereas zinc-free solutions of insulin consist of monomers and dimers.

A series of phase transitions was observed with pH variation, resulting in four distinct polymorphs in the case of cocrystallization with phenol and three polymorphs with resorcinol. In addition to the already known $C222_1$, $C2$ (Norrman & Schluckebier, 2007) and $P2_1$ (Smith *et al.*, 2000) conformations, a new monoclinic phase of insulin has been found (space group $P2_1$). Accurate unit-cell parameters were extracted for all crystalline phases as a function of pH. Human insulin has a remarkably rich phase diagram and polycrystalline precipitates could be obtained and studied under a continuous range of crystallization conditions using powder diffraction.

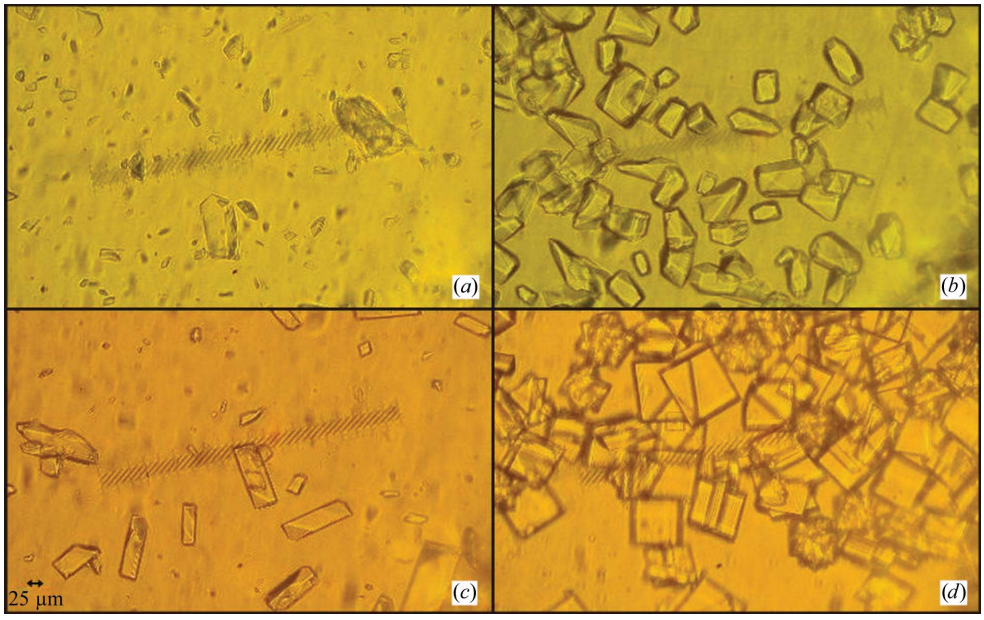

Figure 1
Polycrystalline samples of human insulin cocrystallized with phenol in the four different space groups (*a*) $P2_{1(\alpha)}$, (*b*) $C222_1$, (*c*) $C2$ and (*d*) $P2_{1(\beta)}$ corresponding to pH 5.47, 6.14, 6.75 and 7.46, respectively.

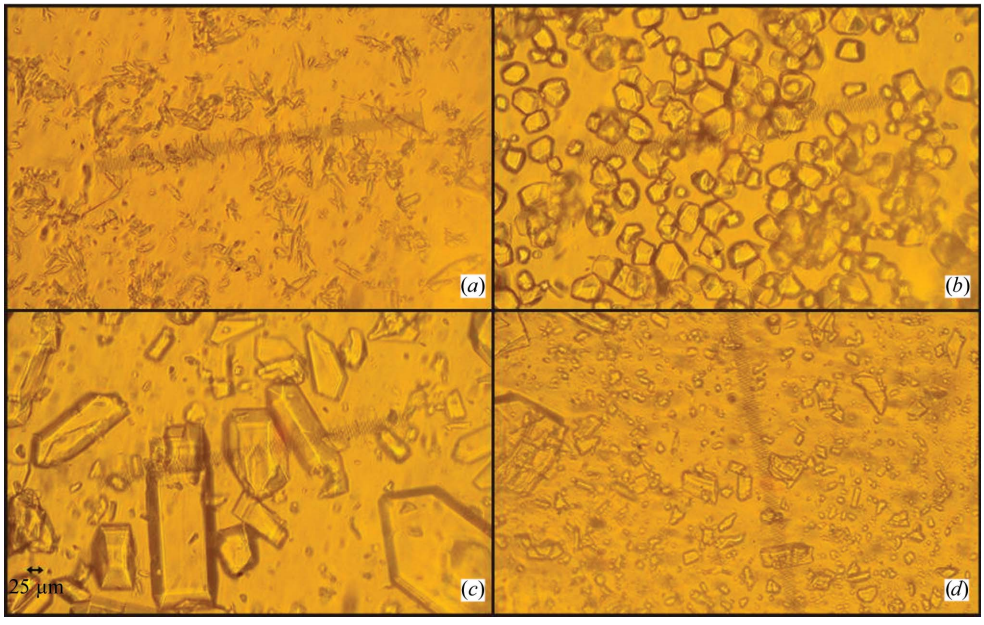

Figure 2
Polycrystalline samples of human insulin cocrystallized with resorcinol in the three different space groups (*a*) $P2_{1(\alpha)}$, (*b*) $C222_1$ and (*c*, *d*) $P2_{1(\beta)}$ corresponding to pH 5.46, 6.40, 7.46 and 8.22, respectively.

2. Experimental

2.1. Crystallization

Human insulin was provided by Novo Nordisk (batch RO10219A). The crystallization method used was the salting-out procedure in batch. The stock protein solution was prepared

by adding 401.2 mg as-received freeze-dried insulin to 21 ml ddH_2O, resulting in a concentration of 17.6 mg ml^{-1}. For the preparation of the protein mixture, 17 ml of the protein solution was extracted and placed in a Falcon tube along with 1.97 ml 0.01 *M* zinc acetate solution and either 0.510 ml 2 *M* phenol diluted in 100% ethanol or 0.255 ml 2 *M* aqueous resorcinol solution. Finally, after 5 min of incubation, 0.255 ml 1 *M* sodium thiocyanate was added to the protein mixture. Furthermore, we prepared two buffer samples of 2 *M* Na_2HPO_4 and KH_2PO_4 that were mixed in order to produce a pH gradient from pH 4.0 to 8.9 with a step of roughly 0.3 units. The NaSCN solution was filtered through 0.22 µm filters and the buffer solutions were filtered with 0.20 µm Filtropur filters before use. In each sample that was produced, 1.2 ml protein mixture and 300 µl pH-buffer mixture were placed in an Eppendorf tube, yielding a final protein concentration of 12.1 mg ml^{-1}. The final resorcinol concentration was 20 m*M*, while the phenol concentration was 41 m*M*. The samples were left to crystallize in an incubator at 298 K. Over the next few days polycrystalline precipitates became visible at the bottom of the Eppendorf tube in each tray, with clear solution above (Figs. 1 and 2). The pH of the crystallization solutions was measured before crystallization as well as after the diffraction experiments and a very small shift toward higher pH values was observed for the majority of the samples. The reported pH levels correspond to the average values of the above measurements.

2.2. X-ray data collection and processing

Powder X-ray diffraction data were collected at room temperature (RT) using a wavelength of 1.299825 (16) Å

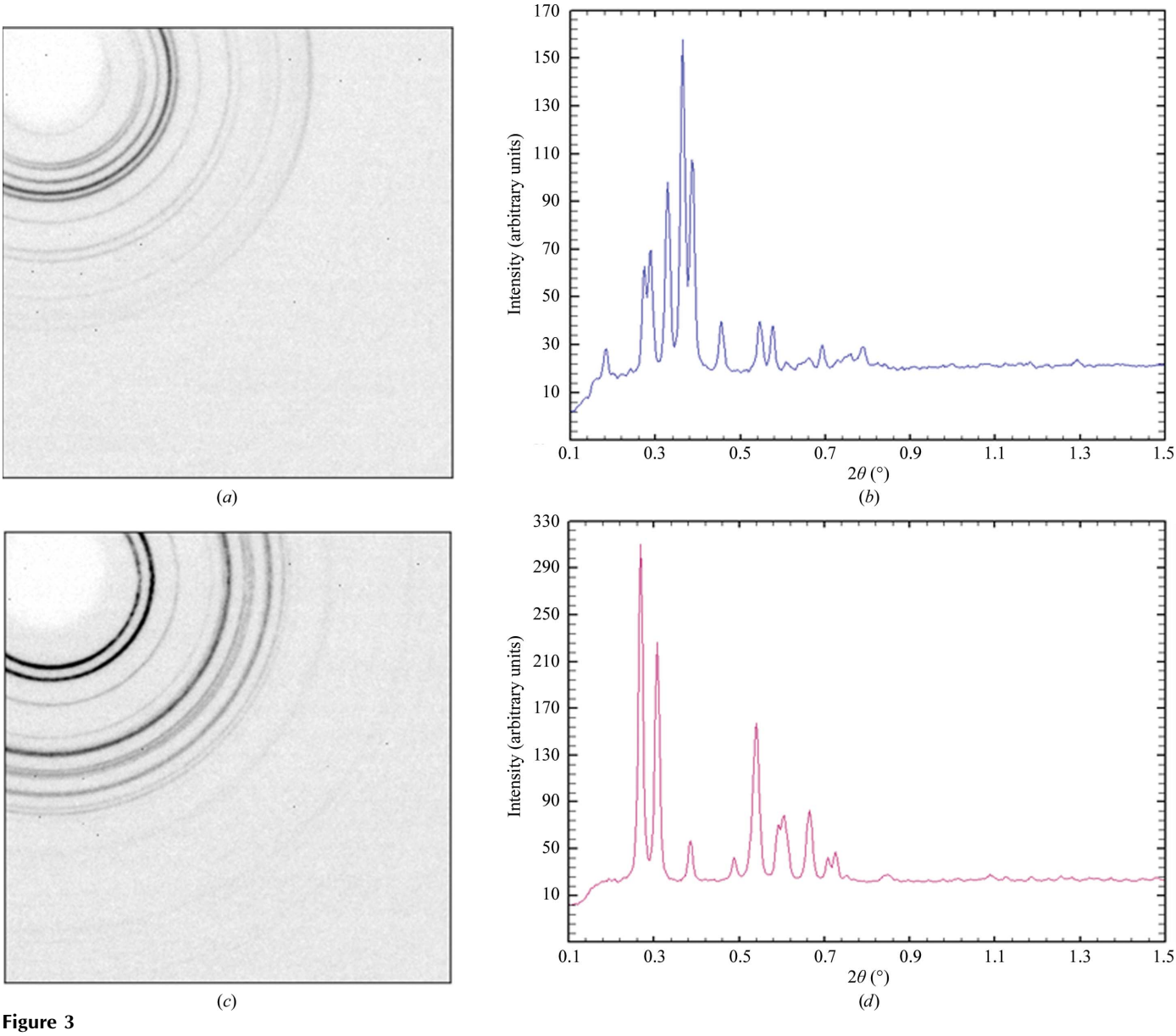

Figure 3
Area-detector images and integrated profiles obtained using the *Fit2D* software of human insulin cocrystallized with phenol at pH 5.75 and 6.78 corresponding to the (*a*, *b*) $P2_{1(\alpha)}$ and (*c*, *d*) $C222_1$ phases. The data were collected at RT [ID11; λ = 0.5339 (5) Å].

Table 1
Refined unit-cell parameters for human insulin cocrystallized with phenol in space groups $P2_{1(\alpha)}$, $C222_1$, $C2$ and $P2_{1(\beta)}$, as extracted from Pawley fits to the experimental data.

pH	Space group	a (Å)	b (Å)	c (Å)	β (°)	Volume (Å^3)	Resolution range (Å)
5.70	$P2_{1(\alpha)}$	114.682 (6)	337.63 (2)	49.270 (4)	101.555 (6)	1869070 (200)	112.2–7.5
6.14	$C222_1$	60.287 (1)	221.797 (6)	228.812 (5)	90	3059560 (117)	115–7.5
6.75	$C2$	103.0115 (5)	61.3213 (2)	63.5783 (4)	117.2244 (5)	357121 (9)	45.9–5.3
7.46	$P2_{1(\beta)}$	61.0920 (4)	61.8279 (4)	47.9302 (4)	110.6253 (7)	169437 (2)	45–4.4

Table 2
Refined unit-cell parameters for human insulin cocrystallized with resorcinol in space groups $P2_{1(\alpha)}$, $C222_1$ and $P2_{1(\beta)}$, as extracted from Pawley fits to the experimental data.

pH	Space group	a (Å)	b (Å)	c (Å)	β (°)	Volume (Å^3)	Resolution range (Å)
5.29	$P2_{1(\alpha)}$	114.0228 (8)	335.430 (3)	49.211 (6)	101.531 (8)	1844227 (293)	112.2–7.5
6.40	$C222_1$	60.5579 (7)	220.907 (3)	228.320 (3)	90	3054394 (63)	115–7.5
8.22	$P2_{1(\beta)}$	61.0008 (4)	62.0040 (3)	47.8823 (3)	110.0465 (5)	170153 (2)	45–4.4

on the high-resolution powder diffraction beamline ID31 at the ESRF, Grenoble (Fitch, 2004). All samples were loaded into 1.0–1.5 mm diameter borosilicate glass capillaries and centrifuged in order to enhance crystal packing. Excess mother liquor was removed and the capillaries were sealed with silicone vacuum grease to prevent dehydration. The capillaries were mounted on the diffractometer and spun at 1000 rev min^{-1} to ensure adequate powder averaging. An automatic sample-changing robot was used for loading and unloading of all of the samples by mounting the capillaries in self-centring magnetic bases. Several scans were collected per sample position, with the capillaries being periodically translated axially to expose a fresh region of sample that was unaffected by the synchrotron beam. Radiation-damage effects are accompanied by marked changes in unit-cell parameters along with gradual increases in peak broadening and can be monitored by comparing the profile measured in each of the nine detector channels during a single scan, as well as by comparing subsequent scans. The first scans, for which the sample had just been translated to expose fresh material, were combined, leading to improved counting statistics without compromising the data quality for structure analysis, while subsequent scans showed detectable degradation and were only employed to follow the evolution of unit-cell parameters with increasing exposure time.

Additional measurements were performed on the materials science beamline ID11 of the ESRF using an area detector. The samples were mounted using both borosilicate glass capillaries (as above) and Kapton capillaries as described by Von Dreele (2006). Data were collected at room temperature. Two subsequent experiments were performed at wavelengths of 0.5339 (5) and 0.3444 (3) Å. The beam was focused using refractive lenses (Vaughan *et al.*, 2011) on the surface of a FReLoN 4M 2k × 2k CCD camera with 50 × 50 µm pixel size (Labiche *et al.*, 2004). The sample-to-detector distance was 794.7 mm and was calibrated using silver behenate (Huang *et*

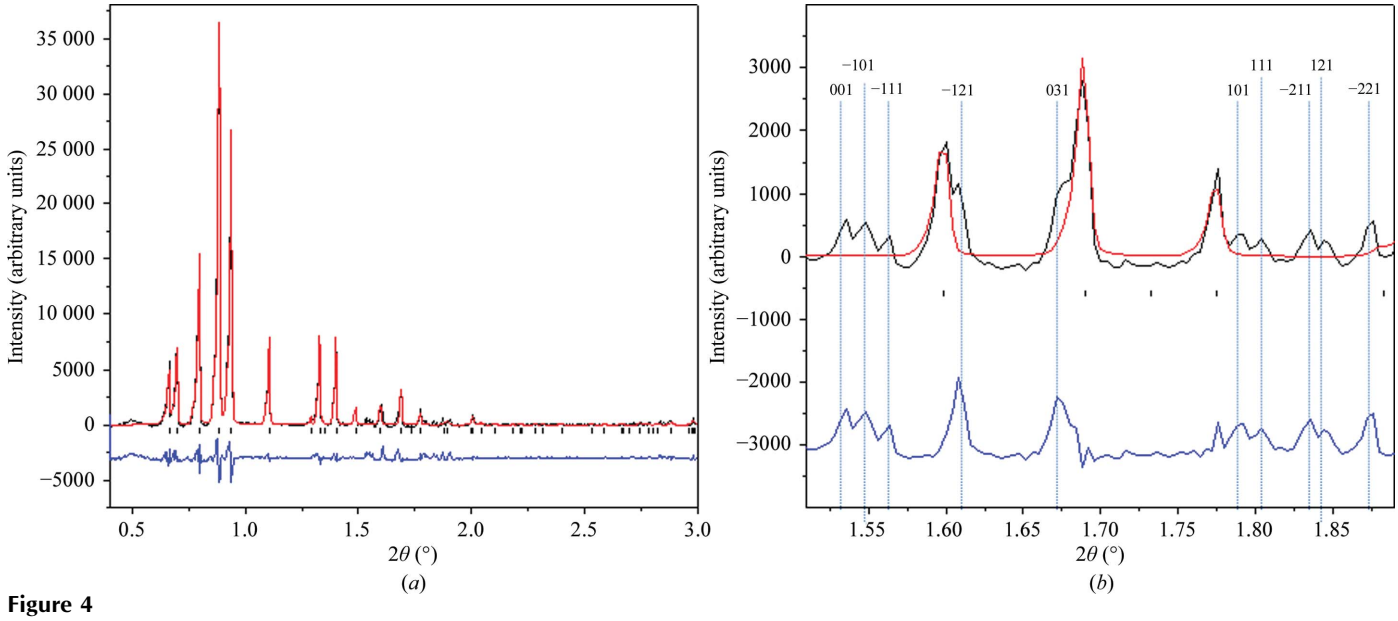

Figure 4
(*a*) Pawley fit of the low-angle region of the $P2_{1(\alpha)}$ polymorph of human insulin cocrystallized with resorcinol at pH 5.46. Owing to the very large b axis and the dominant-zone effect, many reflections may not be observed as a result of peak overlaps. (*b*) Pawley fit of the low-angle peaks in which only the dominant-zone reflections ($hk0$) have been considered and the additional peaks owing to the short c axis are evident. The vertical bars correspond to the theoretical $hk0$ Bragg reflections and the black, red and lower blue lines represent the experimental data, the calculated pattern and the difference between the experimental and calculated profiles, respectively.

al., 1993). A series of images was collected with 1 min exposures at RT. The two-dimensional images were transformed into one-dimensional powder diffraction patterns using *Fit2D* (Hammersley, 1997). Similar patterns were then merged to enhance the counting statistics. The area-detector data (ID11) verified the reproducibility of our high-resolution measurements (ID31) and the sample homogeneity.

In an area-detector image from a crystalline powder sample there is a series of concentric rings, as shown in Fig. 3. Each ring represents the set of reflections corresponding to a particular *d*-spacing in the sample. Smooth rings show that the sample is an ideal powder containing millions of crystallites. Any preferred orientation of the microcrystals would produce intensity variations around the rings, with larger crystallites giving dominant diffraction spots.

The patterns were typically indexed with the *DASH* software package (Boultif & Louër, 1991; David *et al.*, 1998) using the fitted positions of at least the first 20 reflections of the powder diffraction profiles collected from the ID31 samples. From the extracted data, we were able to determine the symmetry and unit-cell parameters. For example, a monoclinic *C*2 unit cell was found for the sample cocrystallized with phenol at pH 6.75, with unit-cell parameters a = 103.0115 (5), b = 61.3213 (2), c = 63.5783 (4) Å, β = 117.2244 (5)°. This phase is in agreement with the monoclinic insulin phase crystallized under similar conditions with the addition of resorcinol and urea at pH 7 (Norrman & Schluckebier, 2007). In order to obtain reliable values of the unit-cell parameters and characterize the peak shape and background coefficients without a structural model, Pawley fits (Pawley, 1981) were performed using the *PRODD* profile-refinement program (Wright, 2004).

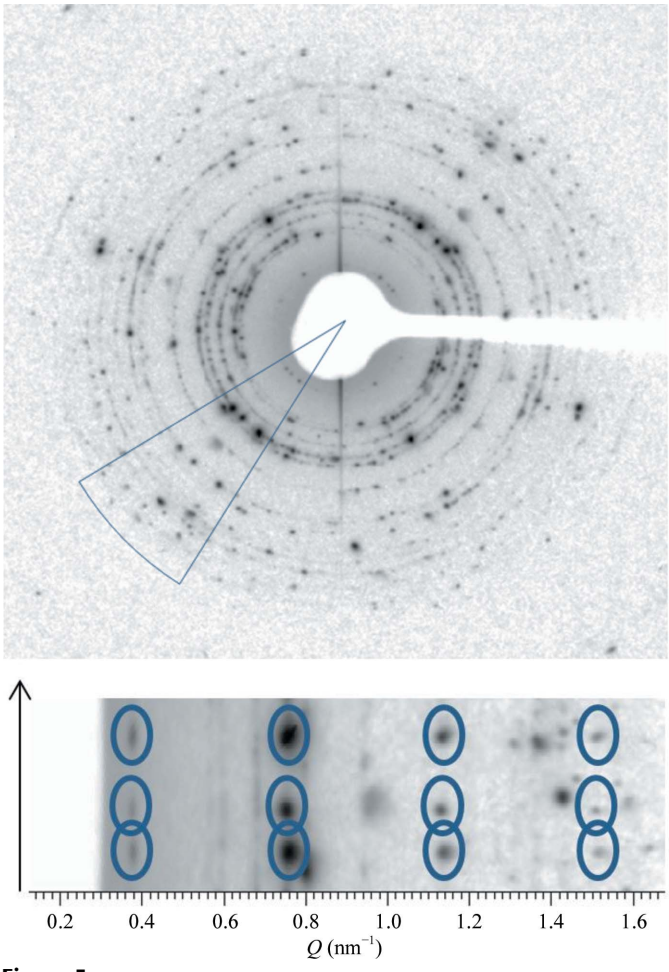

Figure 5
The upper panel shows a two-dimensional image from the sample cocrystallized with resorcinol [pH 5.46, space group $P2_{1(\alpha)}$] in which diffraction spots from single crystals in the sample are visible. In the lower panel, a small region of the data corresponding to the 'cake slice' in the upper panel has been transformed using *Fit2D* to show the intensity *versus* scattering vector Q and azimuthal angle. The (0k0), k = 2n reflections of three different crystals are highlighted by blue circles. The absence of the (030), (050) and (070) reflections suggests that the space group is $P2_{1(\alpha)}$ [ID11, λ = 0.3444 (3) Å].

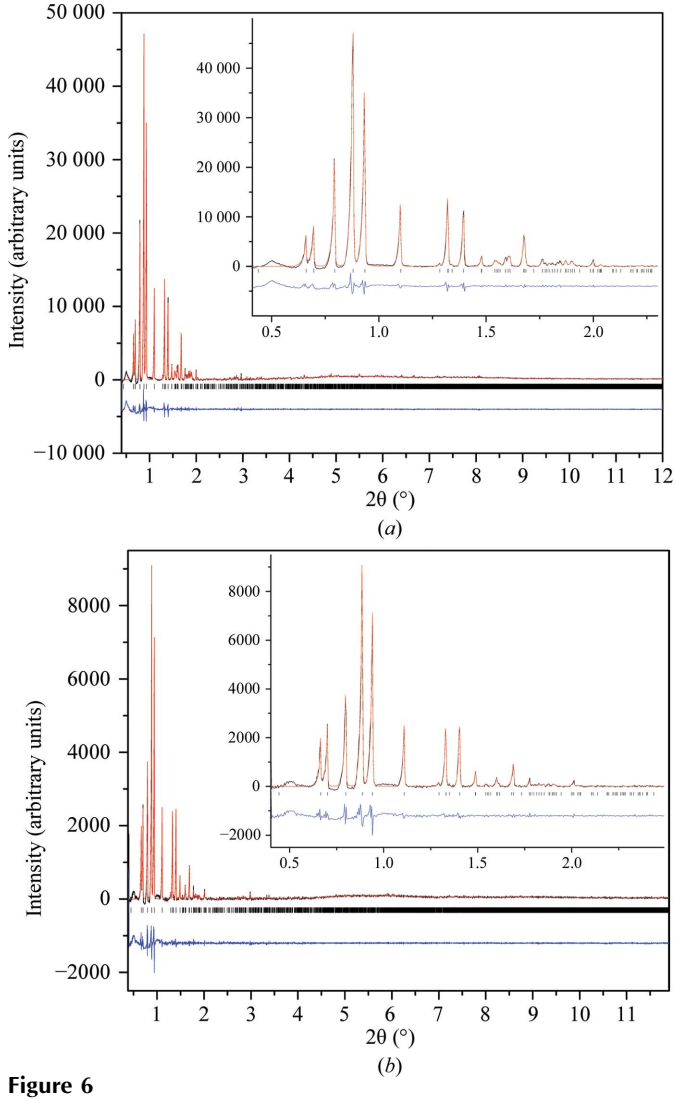

Figure 6
Pawley fit of the novel $P2_{1(\alpha)}$ phase. (*a*) Pawley fit of human insulin cocrystallized with phenol at pH 5.70. (*b*) Pawley fit of human insulin cocrystallized with resorcinol at pH 5.29. All samples were measured using a wavelength of λ = 1.299825 (16) Å. The black, red and lower blue lines represent the experimental data, the calculated pattern and the difference between the experimental and calculated profiles, respectively. The vertical bars correspond to Bragg reflections compatible with this particular space group.

3. Results

The unit-cell parameters of the crystalline phases obtained with phenol and resorcinol with the evolution of pH are presented in Tables 1 and 2.

3.1. Novel monoclinic ($P2_1$) phase *α*

When human insulin was crystallized with phenol in the pH range 5.47–5.70, a novel phase with monoclinic symmetry [space group $P2_1$, referred to in the following as $P2_{1(\alpha)}$] was observed. Owing to the very large *a* and *b* axes in comparison to the *c* axis, the indexing suffered from the dominant-zone problem (Fig. 4). The indexing of such a unit cell is particularly challenging since most of the low-angle reflections belong to the dominant zone in reciprocal space and many reflections may not be observed owing to peak overlap. However, combined use of the ID31 and ID11 data led to the identification of the monoclinic cell $P2_{1(\alpha)}$ with unit-cell parameters a = 114.682 (6), b = 337.63 (2), c = 49.270 (4) Å, β = 101.555 (6)°. The presence of the (020), (040), (060) and (080) reflections and the absence of the (030), (050) and (070) reflections in the ID11 data confirmed the existence of a screw axis (Fig. 5) where spots from individual crystallites are observed, overcoming the powder overlap problem for these reflections. The Pawley fit to the data was satisfactory, with agreement factors of R_{wp} = 3.427 and χ^2 = 2.83 for the sample crystallized at pH 5.7. The data acquired from the $P2_{1(\alpha)}$ crystals extended to a resolution of approximately ∼7.5 Å (Fig. 6). The evolution of the normalized unit-cell parameters is shown in Fig. 7(*a*) and that of the unit-cell volume in shown in Fig. 8(*a*). This is the first report of this specific crystallographic phase of human insulin.

Crystallization of human insulin with resorcinol at pH 5.29 and 5.46 had essentially the same effect as the crystallization screens with phenol and yielded a phase with monoclinic symmetry [space group $P2_1$, unit-cell parameters a = 114.0228 (8), b = 335.43 (3), c = 49.211 (6) Å, β = 101.531 (8)°]. Pawley fits to both data sets were performed

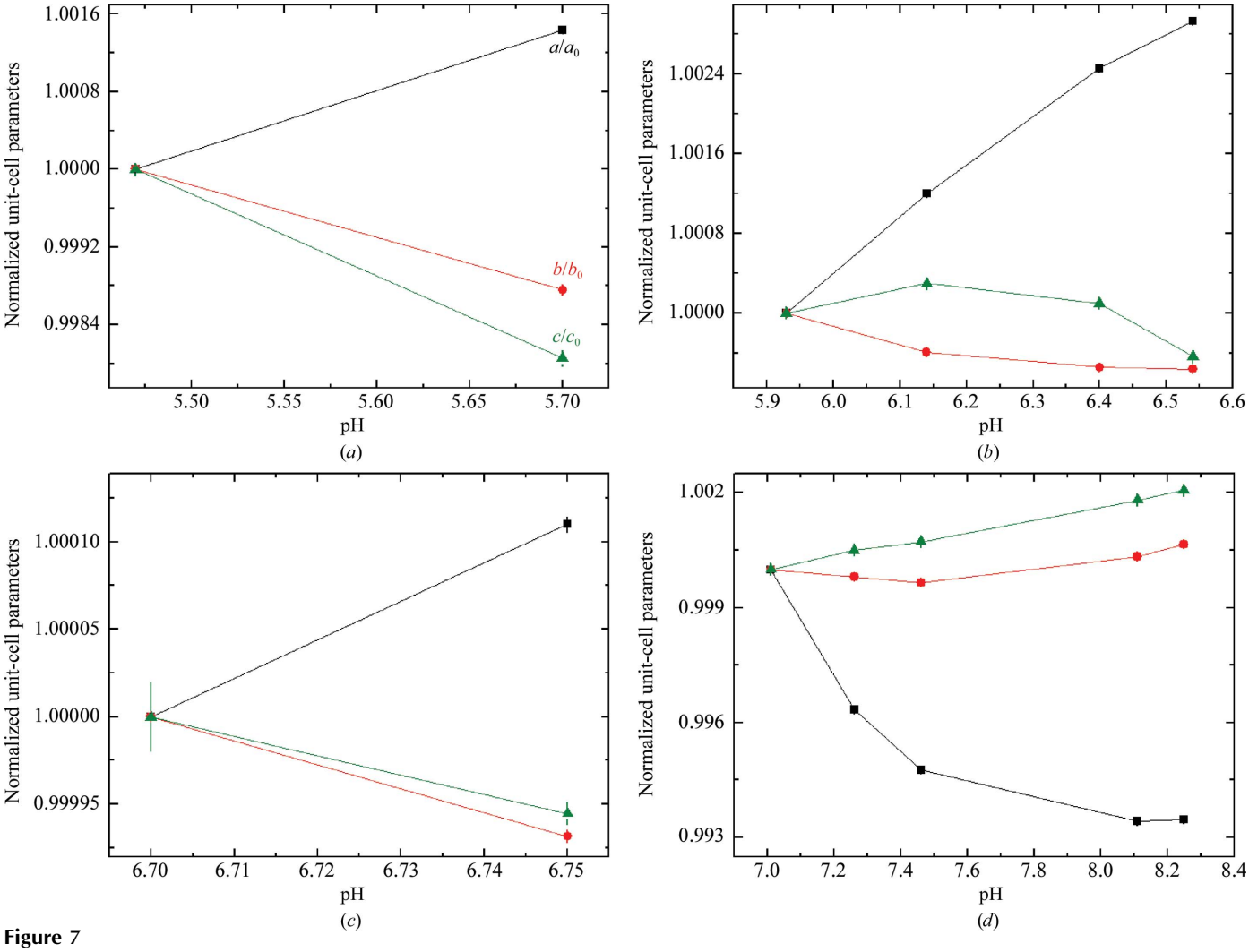

Figure 7
The evolution of the normalized unit-cell parameters of human insulin cocrystallized with phenol with increasing pH for space groups (*a*) $P2_{1(\alpha)}$, (*b*) $C222_1$, (*c*) $C2$ and (*d*) $P2_{1(\beta)}$. The black symbols correspond to the *a* axis of the unit cell, the red symbols to the *b* axis and the green symbols to the *c* axis. a_0, b_0 and c_0 correspond to the refined values at the first pH where each crystalline phase was identified. The values are listed in Supplementary Table S1. The lines are a guide to the eye.

in order to extract accurate unit-cell parameters, resulting in acceptable agreement factors (R_{wp} = 5.7 and χ^2 = 1.58 for a sample crystallized at pH 5.29). Data obtained from these samples extended to a resolution of ∼7.5 Å (Fig. 6). The increase in pH from 5.29 to 5.46 resulted in a slight increase in the unit-cell volume ($\Delta V/V_i$ = 0.29%). Furthermore, the unit-cell parameters of the samples with phenol indicated a larger unit cell than the samples with resorcinol. Structure solution is necessary in order to identify the exact positions of the ligand-binding sites and the effect on the volume of the monoclinic unit cell. The evolution of the normalized unit-cell parameters with pH is shown in Fig. 9(*a*) and that of the unit-cell volume is shown in Fig. 8(*b*).

3.2. Orthorhombic ($C222_1$) phase

Human insulin crystallized in the presence of phenol in the slightly higher pH range of 5.93–6.54 and of resorcinol in the slightly higher pH range of 5.93–7.45 produced crystals with orthorhombic symmetry (space group $C222_1$; see Tables 1 and 2 for unit-cell parameters) containing three protein hexamers per asymmetric unit (Norrman & Schluckebier, 2007). The data obtained from these samples extended to a resolution of ∼7.5 Å (Fig. 10*a*). In both cases, the increase in pH resulted in minor alterations of the unit-cell parameters and no indication of a first-order phase transition. In the case of phenol, this specific variation of pH led to a slight increase in the unit-cell volume ($\Delta V/V_i$ = 0.19%) and in the case of resorcinol there was an increase of $\Delta V/V_i$ = 0.83%. The unit-cell parameters of this phase are in good agreement with the structural models

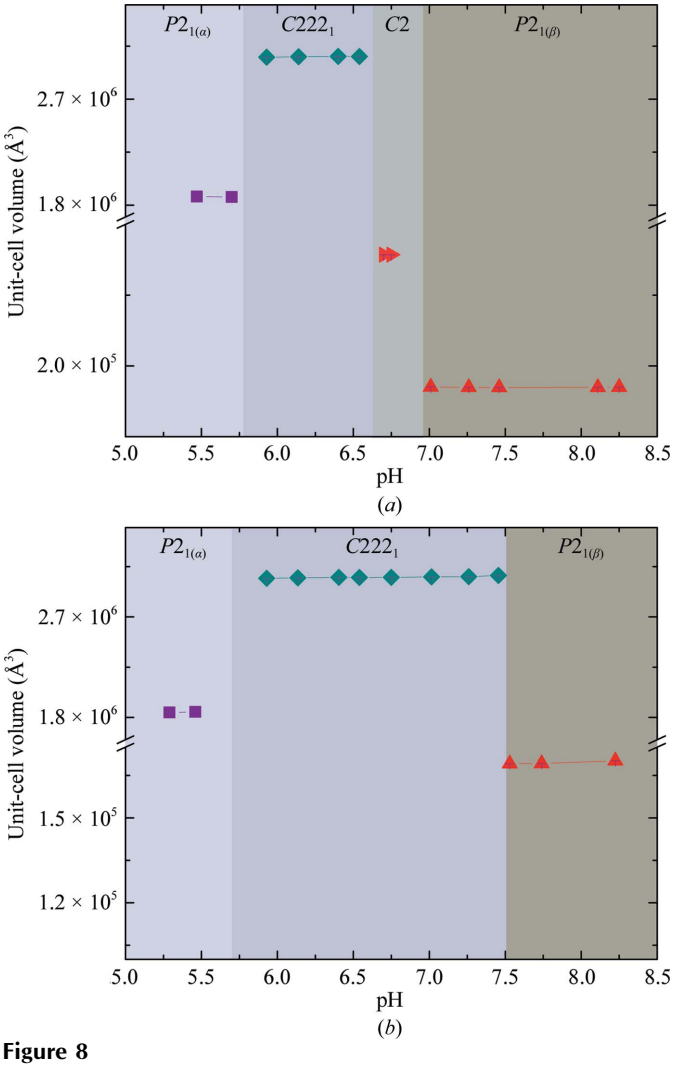

Figure 8
Evolution of the unit-cell volume with pH for insulin cocrystallized with (*a*) phenol and (*b*) resorcinol in each corresponding crystalline phase.

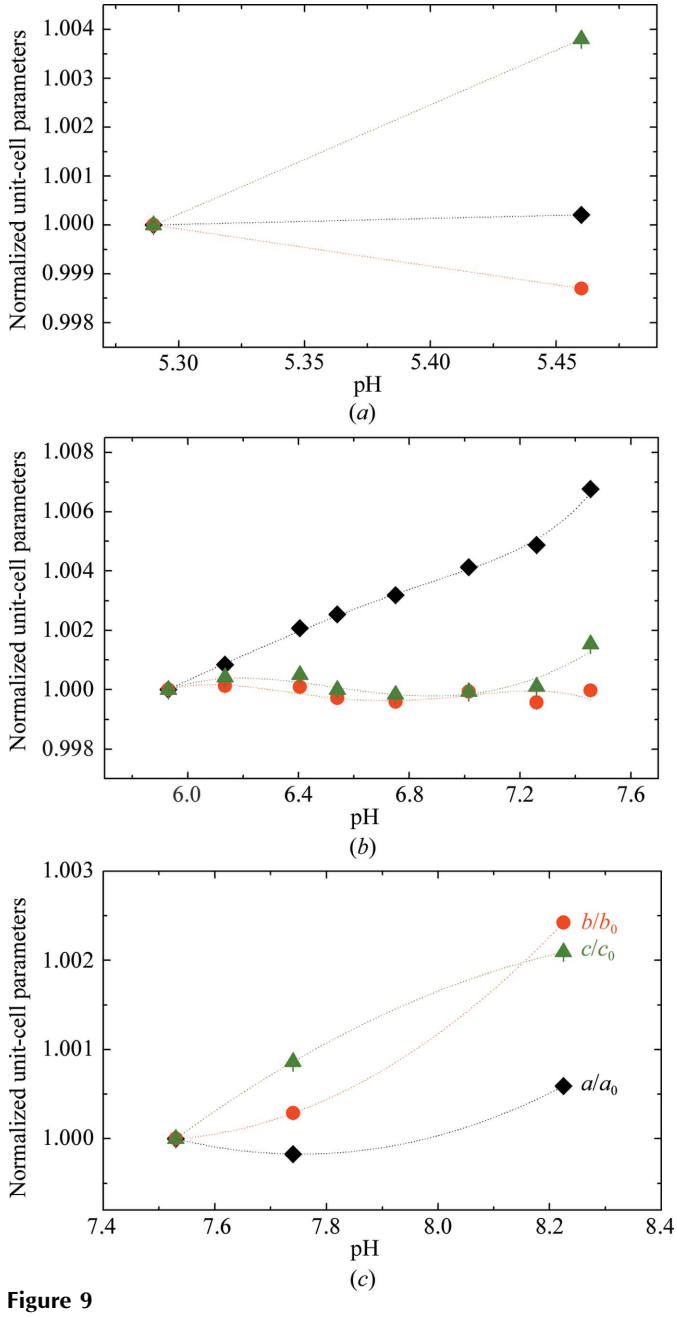

Figure 9
Evolution of the normalized unit-cell parameters of human insulin cocrystallized with resorcinol with increasing pH for space groups (*a*) $P2_{1(\alpha)}$, (*b*) $C222_1$ and (*c*) $P2_{1(\beta)}$. The black symbols correspond to the *a* axis of the unit cell, the red symbols to the *b* axis and the green symbols to the *c* axis. a_0, b_0 and c_0 correspond to the refined values at the first pH where each crystalline phase was identified. The values are listed in Supplementary Table S2[1]. The lines are a guide to the eye.

reported previously with PDB codes 2om0 and 2om1 (Norrman & Schluckebier, 2007). At pH 5.7 and in the presence of resorcinol the $P2_{1(\alpha)}$ and $C222_1$ phases co-exist. Consequently, the transition from the first crystal type to the second crystal type causes a volume modification of about $\Delta V_{[P2_{1(\alpha)}\rightarrow C222_1]}/V_{[P2_{1(\alpha)}]}$ = 64.70%. The evolution of the normalized unit-cell parameters for human insulin with phenol and resorcinol is illustrated in Figs. 7(*b*) and 9(*b*), respectively.

3.3. Monoclinic (*C*2) phase

Two samples of insulin crystallized in the presence of phenol at pH 6.70 and 6.75 were found to belong to the monoclinic space group *C*2 (see Table 1) containing one protein hexamer per asymmetric unit. The data for this phase extended to a resolution of ∼5.3 Å (Fig. 10*b*) and the results showed that the *C*2 phase has a smaller unit-cell volume compared with the $C222_1$ crystals as a result of the large change of the unit-cell parameters. This change resulted in a significant reduction in the unit-cell volume by approximately $\Delta V_{(C222_1\rightarrow C2)}/V_i$ = −88.33% as the space group changed from $C222_1$ to *C*2. The evolution of the normalized unit-cell parameters is shown in Fig. 7(*c*). The unit-cell parameters of this model were very similar to those of models 2oly and 2olz available in the PDB (Norrman & Schluckebier, 2007). The evolution of the unit-cell volume is shown in Fig. 8(*a*).

3.4. Monoclinic ($P2_1$) phase *β*

Samples of human insulin cocrystallized at higher pH values with phenol (pH 7.01–8.25) and resorcinol (pH 7.53–8.22) caused the formation of crystals with monoclinic symmetry [$P2_1$, referred to in the following as $P2_{1(\beta)}$; see Tables 1 and 2] with one protein hexamer in the asymmetric unit. The data resolution of these samples extended to approximately ∼4.4 Å (Fig. 10*c*). This phase has the smallest unit-cell volume of all of the insulin/phenol polymorphs reported in this study, with the volume decreasing by $\Delta V_{[C2\rightarrow P2_{1(\beta)}]}/V_{(C2)}$ = −52.35% during the phase transition between *C*2 and $P2_{1(\beta)}$. According to Matthews coefficient calculation (Matthews, 1968; Kantardjieff & Rupp, 2003), the *C*2 phase contains four hexamers per unit cell with 52% solvent content (Matthews coefficient = 2.56 Å^3 Da^{-1}), whereas the $P2_{1(\beta)}$ phase contains two hexamers per unit cell with 49.4% solvent content (Matthews coefficient = 2.43 Å^3 Da^{-1}). Furthermore, there is a very small decrease in the unit-cell volume within this pH range ($\Delta V/V_i$ = −0.22%), which is reflected in the slightly anisotropic unit-cell parameter evolution observed with the increase in pH (see Table 3). This result might be indicative of solvent rearrangement, slight changes of the protein conformation or changes

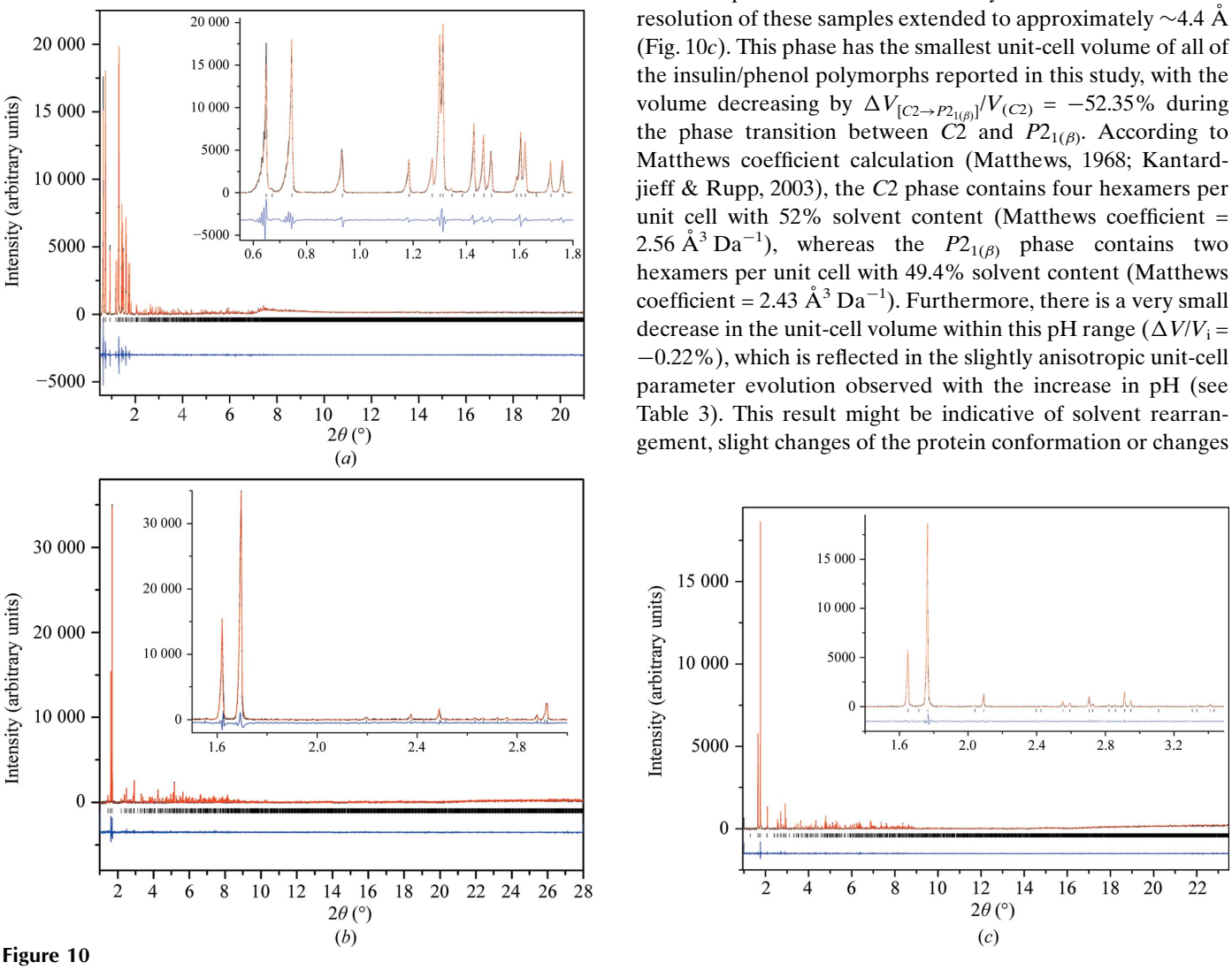

Figure 10
Pawley fits of three different phases of human insulin cocrystallized under various conditions. (*a*) Pawley fit of the $C222_1$ phase of human insulin cocrystallized with resorcinol at pH 6.40, (*b*) Pawley fit of the *C*2 phase of human insulin cocrystallized with phenol at pH 6.75 and (*c*) Pawley fit of the $P2_{1(\beta)}$ phase of human insulin cocrystallized with resorcinol at pH 8.22. All samples were measured using a wavelength of λ = 1.299825 (16) Å. The black, red and lower blue lines represent the experimental data, the calculated pattern and the difference between the experimental and calculated profiles, respectively. The vertical bars correspond to Bragg reflections compatible with this particular space group. The inset corresponds to a magnification of the fit in the selected 2*θ* range.

Table 3
Summary of alterations in the unit-cell parameters of the $P2_{1(\alpha)}$, $C222_1$, $C2$ and $P2_{1(\beta)}$ polymorphs with increasing pH.

We note that the $C2$ polymorph is not present in any of the human insulin–resorcinol complexes.

Polymorph	$P2_{1(\alpha)}$		$C222_1$		$C2$	$P2_{1(\beta)}$	
Ligand	Phenol	Resorcinol	Phenol	Resorcinol	Phenol	Phenol	Resorcinol
$\Delta a/a_i$ (%)	0.14	0.02	0.29	0.68	0.01	−0.65	0.05
$\Delta b/b_i$ (%)	−0.12	−0.13	−0.06	−0.002	−0.01	0.07	0.24
$\Delta c/c_i$ (%)	−0.19	0.38	−0.04	0.15	−0.006	0.21	0.21
$\Delta\beta/\beta_i$ (%)	0.11	0.004	—	—	0.02	−0.22	−0.13
ΔpH	0.23	0.17	0.61	1.53	0.05	1.24	0.69
$\Delta V/V_i$ (%)	0.21	0.29	0.19	0.83	0.03	−0.22	0.60
$(\Delta V/V_i)/\Delta$pH (%)	0.91	1.71	0.31	0.54	0.54	−0.18	0.87

in packing contacts. In the case of cocrystallization with resorcinol there is also a very small increase in the unit-cell volume *within* the space group, $\Delta V/V_i = 0.604\%$, which is reflected in the slightly anisotropic unit-cell parameter evolution observed with the increase in pH (Table 3). The unit-cell parameters of this phase closely matched those of PDB entries 1evr and 1ev6 (Smith *et al.*, 2000). The evolution of the normalized unit-cell parameters with pH is shown in Figs. 7(*d*) and 9(*c*) for phenol and resorcinol, respectively.

4. Discussion

Polymorphism of molecular crystals is an important and well researched field (Bernstein, 2002). For macromolecular crystals, insulin serves as a model system owing to its biomedical and pharmacological importance and the long history of research on its crystallization (Abel, 1926; Krayenbüh & Rosenberg, 1946; Schlichtkrull, 1958; Brange *et al.*, 1992). For wild-type human insulin, a large number of different crystal polymorphs have been identified over the last 80 years and are often associated with different self-association and allosteric states of the insulin molecule (Kaarsholm *et al.*, 1989; Ciszak & Smith, 1994; Smith *et al.*, 2005).

Microcrystalline insulin suspensions remain the most widely used pharmaceutical insulin preparations owing to their stability and their protracted action profile (Brange *et al.*, 1992), even though they have been available for more than 50 years. These pharmaceutical preparations contain insulin, zinc and a phenolic ligand. Knowledge of the crystallization properties of such mixtures will on the one hand aid in the optimization of production processes, but may also lead to the development of novel insulin preparations for alternative delivery, such as sustained-release formulations or pulmonary delivery (Basu *et al.*, 2004), as the choice of the correct polymorph influences properties such as the stability, solubility and bioavailability of insulin crystals.

Here, we have undertaken a systematic study of the effect of pH on the crystallization behaviour of insulin in complex with zinc, the stabilizing zinc ligand thiocyanate and a phenolic ligand, with the surprising and unexpected discovery of a preivously undescribed crystal form of insulin.

In the present study, our primary focus is to examine the effects of pH in addition to cocrystallization with the small organic ligands phenol and resorcinol on the obtained crystal motifs of human insulin. We have made accurate measurements of the evolution of the unit-cell parameters with pH, which are illustrated by the smooth anisotropic shifts in the peak positions. Furthermore, the reproducibility of these results and the precision of the powder diffraction data have been verified by carrying out multiple crystallization and diffraction experiments at room temperature. The results obtained using different instrumental configurations for improving data accuracy have been discussed elsewhere (Margiolaki *et al.*, 2007; Margiolaki & Wright, 2008; Margiolaki, 2013). High-resolution powder diffraction measurements have revealed seven distinct phases in total, which correspond to four packing arrangements [$P2_{1(\alpha)}$, $C222_1$, $C2$ and $P2_{1(\beta)}$]. The results show that human insulin crystallized in the presence of phenol and resorcinol can be greatly affected by pH. Distinct polymorphs characterized by altered crystallographic symmetries and/or unit-cell parameters were obtained depending on the pH value (Tables 1 and 2). Insulin crystallized with either of the ligands at an approximate pH of 5.5 forms crystals that assume the novel $P2_{1(\alpha)}$ symmetry, as shown by the presented data. With the exception of the $C2$ phase, which was only observed on cocrystallization with phenol, the rest of the phases obtained coincided in the two crystallization experiments. Although phenol and resorcinol can substitute for each other as allosteric ligands of the insulin hexamer without detectable changes in insulin structure (Smith *et al.*, 2000), the choice of ligand apparently influences the crystallization behavior. This is noteworthy, as the phenolic binding site is buried and does not contribute to crystal contacts. The complete unit-cell parameters of the crystalline phases obtained with phenol and resorcinol with the evolution of pH are presented in Supplementary Tables S1 and S2.[1]

Our results demonstrate that systematic screening of crystallization conditions in combination with synchrotron X-ray powder diffraction yields an exact and unambiguous picture of the crystallization behaviour of insulin even around its pI (∼5.9), where its solubility is lowest and the growth of

[1] Supplementary material has been deposited in the IUCr electronic archive (Reference: DW5028). Services for accessing this material are described at the back of the journal.

macroscopic crystals suitable for single-crystal X-ray structure determination is least likely to succeed.

We believe that this kind of systematic approach further extends the applicability of powder diffraction methods for systematic macromolecular crystal screening in a wide range of crystallization conditions. The low instrumental contribution to the diffraction lines and the high precision of the determination of unit-cell parameters allowed small variations of the unit-cell parameters to be quantified precisely. The use of systematic variation of sample-preparation conditions is likely to be particularly useful for the detection of protein–ligand complex formation by variations of ligand concentration (Von Dreele, 2001, 2005).

We would like to thank the ESRF for provision of beam time at the ID31 and ID11 beamlines and Novo Nordisk S/A for the provision of human insulin and their valuable advice on crystallization procedures. IM is grateful to the Unesco L'Oreal foundations for the award of the International Fellowship for Women in Life Sciences (2010). This research was co-financed by the European Union (European Regional Development Fund; ERDF) and Greek National Funds through the Operational Programme 'Regional Operational Programme' of the National Strategic Reference Framework (NSRF) Research Funding Programme Support for Research, Technology and Innovation Actions in Region of Western Greece. Finally, the EU FP7 REGPOT CT-2011-285950 'SEE-DRUG' project supported this work.

References

Abel, J. J. (1926). *Proc. Natl Acad. Sci. USA*, **12**, 132–136.
Adams, M. J., Blundell, T. L., Dodson, E. J., Dodson, G. G., Vijayan, M., Baker, E. N., Harding, M. M., Hodgkin, D. C., Rimmer, B. & Sheat, S. (1969). *Nature (London)*, **224**, 491–495.
Banting, F. G. & Best, C. H. (1922). *J. Lab. Clin. Med.* **7**, 251–266.
Basso, S., Fitch, A. N., Fox, G. C., Margiolaki, I. & Wright, J. P. (2005). *Acta Cryst.* D**61**, 1612–1625.
Basu, S. K., Govardhan, C. P., Jung, C. W. & Margolin, A. L. (2004). *Expert Opin. Biol. Ther.* **4**, 301–317.
Bernstein, J. (2002). *Polymorphism in Molecular Crystals.* Oxford University Press.
Boultif, A. & Louër, D. (1991). *J. Appl. Cryst.* **24**, 987–993.
Brange, J., Langkjaer, L., Havelund, S. & Vølund, A. (1992). *Pharm. Res.* **9**, 715–726.
Ciszak, E. & Smith, G. D. (1994). *Biochemistry*, **33**, 1512–1517.
Collings, I., Watier, Y., Giffard, M., Dagogo, S., Kahn, R., Bonneté, F., Wright, J. P., Fitch, A. N. & Margiolaki, I. (2010). *Acta Cryst.* D**66**, 539–548.
David, W. I. F., Shankland, K. & Shankland, N. (1998). *Chem. Commun.*, pp. 931–932.
Derewenda, U., Derewenda, Z., Dodson, E. J., Dodson, G. G., Reynolds, C. D., Smith, G. D., Sparks, C. & Swenson, D. (1989). *Nature (London)*, **338**, 594–596.
Fitch, A. N. (2004). *J. Res. Natl Inst. Stand. Technol.* **109**, 133–142.
Hammersley, A. P. (1997). ESRF Internal Report ESRF 97HA02T.
Huang, T. C., Toraya, H., Blanton, T. N. & Wu, Y. (1993). *J. Appl. Cryst.* **26**, 180–184.
Itoh, N. & Okamoto, H. (1980). *Nature (London)*, **283**, 100–102.
Kaarsholm, N. C., Ko, H. C. & Dunn, M. F. (1989). *Biochemistry*, **28**, 4427–4435.
Kantardjieff, K. A. & Rupp, B. (2003). *Protein Sci.* **12**, 1805–1871.
Krayenbüh, C. & Rosenberg, T. (1946). *Rep. Steno. Mem. Hosp. Nord. Insulinlab.* **1**, 60–73.
Labiche, J. C., Mathon, O., Pascarelli, S., Newton, M. A., Ferre, G. G., Curfs, C., Vaughan, G., Larson, A. C. & Von Dreele, R. B. (2004). Los Alamos National Laboratory Report LAUR 86-748.
Leibowitz, G., Uçkaya, G., Oprescu, A. I., Cerasi, E., Gross, D. J. & Kaiser, N. (2002). *Endocrinology*, **143**, 3214–3220.
Margiolaki, I. & Wright, J. P. (2008). *Acta Cryst.* A**64**, 169–180.
Margiolaki, I., Wright, J. P., Fitch, A. N., Fox, G. C., Labrador, A., Von Dreele, R. B., Miura, K., Gozzo, F., Schiltz, M., Besnard, C., Camus, F., Pattison, P., Beckers, D. & Degen, T. (2007). *Z. Kristallogr. Suppl.* **26**, 1–13.
Margiolaki, I., Wright, J. P., Fitch, A. N., Fox, G. C. & Von Dreele, R. B. (2005). *Acta Cryst.* D**61**, 423–432.
Margiolaki, I. (2013). *International Tables for Crystallography*, Vol. *H*. In the press.
Matthews, B. W. (1968). *J. Mol. Biol.* **33**, 491–497.
Norrman, M. (2007). PhD thesis. Lund University, Sweden.
Norrman, M. & Schluckebier, G. (2007). *BMC Struct. Biol.* **7**, 83.
Norrman, M., Ståhl, K., Schluckebier, G. & Al-Karadaghi, S. (2006). *J. Appl. Cryst.* **39**, 391–400.
Pawley, G. S. (1981). *J. Appl. Cryst.* **14**, 357–361.
Schlichtkrull, J. (1958). *Insulin Crystals.* Copenhagen: Munksgaard.
Smith, G. D., Ciszak, E., Magrum, L. A., Pangborn, W. A. & Blessing, R. H. (2000). *Acta Cryst.* D**56**, 1541–1548.
Smith, G. D., Pangborn, W. A. & Blessing, R. H. (2005). *Acta Cryst.* D**61**, 1476–1482.
Vaughan, G. B. M., Wright, J. P., Bytchkov, A., Rossat, M., Gleyzolle, H., Snigireva, I. & Snigirev, A. (2011). *J. Synchrotron Rad.* **18**, 125–133.
Von Dreele, R. B. (1999). *J. Appl. Cryst.* **32**, 1084–1089.
Von Dreele, R. B. (2001). *Acta Cryst.* D**57**, 1836–1842.
Von Dreele, R. B. (2003). *Methods Enzymol.* **368**, 254–267.
Von Dreele, R. B. (2005). *Acta Cryst.* D**61**, 22–32.
Von Dreele, R. B. (2006). *J. Appl. Cryst.* **39**, 124–126.
Von Dreele, R. B., Stephens, P. W., Smith, G. D. & Blessing, R. H. (2000). *Acta Cryst.* D**56**, 1549–1553.
Wright, J. P. (2004). *Z. Kristallogr.* **219**, 791–802.
Wright, J. P., Besnard, C., Margiolaki, I., Basso, S., Camus, F., Fitch, A. N., Fox, G. C., Pattison, P. & Schiltz, M. (2008). *J. Appl. Cryst.* **41**, 329–339.